Engineered Whole Cut Meats Assembled of Cell Fibers Constructed by Tendon-Gel Integrated Bioprinting

Dong-Hee Kang
Osaka University
Fiona Louis
Osaka University
Hao Liu
Osaka University
Hiroshi Shimoda
Hirosaki University Graduate School of Medicine
Yasutaka Nishiyama
Nipponham Foods, Ltd
Hajime Nozawa
Kirin Holdings Company, Limited
Makoto Kakitani
Kirin Holdings Company, Limited
Daisuke Takagi
Ricoh Company, Ltd
Daijiro Kasa
Ricoh Japan Corporation
Eiji Nagamori
Osaka Institute of Technology
Shinji Irie
Toppan Printing CO., LTD
Shiro Kitano
Toppan Printing CO., LTD
Michiya Matsusaki (m-matsus@chem.eng.osaka-u.ac.jp)
Osaka University https://orcid.org/0000-0003-4294-9313

Biological Sciences - Article

Keywords: Engineered steak-like meat, Tendon-integrated bioprinting, Cell fibers

Posted Date: October 16th, 2020

DOI: https://doi.org/10.21203/rs.3.rs-91978/v1

Engineered Whole Cut Meats Assembled of Cell Fibers Constructed by Tendon-Gel Integrated Bioprinting

*Dong-Hee Kang[1], Fiona Louis[2], Hao Liu[1], Hiroshi Shimoda[3], Yasutaka Nishiyama[4], Hajime Nozawa[5], Makoto Kakitani[5], Daisuke Takagi[6], Daijiro Kasa[7], Eiji Nagamori[8], Shinji Irie[2], Shiro Kitano[2], and Michiya Matsusaki[1,2]**

[1]Division of Applied Chemistry, Graduate School of Engineering, Osaka University, 2-1 Yamadaoka, Suita, Osaka 565-0871, Japan

[2]Joint Research Laboratory (TOPPAN) for Advanced Cell Regulatory Chemistry, Graduate School of Engineering, Osaka University, 2-1 Yamadaoka, Suita, Osaka 565-0871, Japan

[3]Department of Anatomical Science, Hirosaki University Graduate School of Medicine, 5 Zaifu-cho, Hirosaki, 036-8562, Japan.

[4]Nipponham Foods, Ltd., 3-3 Midorigahara, Tsukuba, Ibaraki 300-2646, Japan.

[5]Cell Therapy Project, Research & Development Division, Kirin Holdings Company, Limited, 1-13-5, Fukuura, Kanazawa-ku, Yokohama 236-0004, Japan.

[6]Biomedical Business Center, Healthcare Business Group, Ricoh Company, Ltd., 3-25-22 Tonomachi LIC 322, Kawasaki-shi, Kanagawa 210-0821, Japan.

[7]Solution Planning, Product Solution Technologies, Production Printing, Industrial Solutions, Ricoh Japan Corporation, 4-2-8 Shibaura, Minato-ku, Tokyo 108-0023, Japan.

[8]Department of Biomedical Engineering, Faculty of Engineering, Osaka Institute of Technology, 5-16-1 Omiya, Asahi-ku, Osaka 535-8585, Japan

*Corresponding author foot note:
Professor Michiya Matsusaki, PhD
E-mail: m-matsus@chem.eng.osaka-u.ac.jp

Keywords: Engineered steak-like meat, Tendon-integrated bioprinting, Cell fibers

Abstract

With the current interest in artificial meat, mammalian cell-based cultured meat has mostly been in minced form. There is thus still a high demand for artificial steak-like meat. Herein, we demonstrate *in vitro* construction of engineered steak-like meat assembled of three types of edible bovine cell fibers, such as skeletal muscle, adipose, and blood capillary fabricated by tendon-gel integrated printing (TIP) technology. Because actual meat is an anisotropically aligned assembly of the fibers connected to tendon for the actions of contraction and relaxation, TIP was discovered to construct the fiber assembly connecting tendon gels with engineered structures. In this study, a total of 72 fibers comprising 42 muscle, 28 adipose, and 2 blood capillary were constructed by TIP and subsequently assembled to fabricate a steak-like meat with a diameter of 5 mm and a length of 10 mm by consulting histological images of actual Wagyu beef steak. The TIP discovered here could be a powerful manufacturing technology for fabrication of the desired types of steak-like cultured meats.

Introduction

Over the past decade, cultured meat has drawn tremendous attention from standpoints of ethics, economics, the environment, and public health. More recently, meat analogs that taste like meat but are based on plant proteins have been released commercially[1,2]. Although challenges remain unlike with meat analogs, cultured meat is highly sought after due to the possibility of imitating real meat through the manipulation of flavor, muscle/adipose cells ratio, and texture[3,4]. Bovine cells for cultured meat can currently be secured by two approaches[5,6]. One is that after obtaining edible tissues from cattle, they are separated into each cell type such as muscle satellite cells, adult stem cells, and multipotent stem cells etc. which are then cultured to increase the number of cells. The other is to transform somatic cells into induced pluripotent stem cells (iPSCs) and differentiate to each cell type. Even though primary cultured stem cells, particularly muscle satellite cells that maintain the differentiation capability within 10 passage[7], have a limited number of divisions, they would still be safe and acceptable for consumption. Edible forms can also be constructed by the assembly of acquired bovine cells. Since Post and co-workers unveiled minced meat composed of lab-grown bovine cells, various types of cultured meat have been demonstrated. However, cultured steak with a compositional and structural similarity to real steak, comprising mostly muscle and adipose cells with muscle cells in alignment, is still challenging[4,8,9].

To realize the structural characteristics of steak, various tissue engineering techniques have been considered such as cell sheet engineering[10,11], cell fiber engineering[12], cell culture on a 3D printed scaffold[13], and 3D cell printing[14,15]. It is noteworthy that in the 3D cell printing field some researchers have adopted a supporting bath assisted 3D printing (SBP) technique where ink is dispensed inside the gel or suspensions with thixotropy. Since the SBP is able to overcome the shortcomings of restricted available range of viscosity in ink and drying for

prolonged printing in extrusion-based 3D printing on the air-interfaced environment, several studies over the past 5 years have shown evidence of its potential in a complex tissue fabrication[16–22].

Steak meat is an aligned assembly of skeletal muscle fascicles with a diameter from around 900 μm to 2.3 mm[23] depending on age and animal parts, which are the assembly of skeletal muscle fibers, connecting to tendon for the movements of its shrinkage and relaxation. The muscle fibers are covered with basement membrane and the muscle fascicles are surrounded by fat together with blood capillaries (Fig. 1a). The component ratio and location of the muscle, adipose, and blood capillary tissues are significantly different according to meat type and original country of origin. For example, red meat in the rump of Japanese Wagyu has only 10.7% adipose tissues, whereas the sirloin of the Wagyu has 47.5%[24]. Accordingly, development of a novel methodology for assembling the three types of fibers with desired location, ratio, and amount will be a key manufacturing technology of cultured steak.

Here, we demonstrate a three-step strategy for the construction of engineered steak-like meat: (1) Collection of edible bovine satellite cells (bSCs) and adipose-derived stem cells (bADSCs) from approved block beef meats and subsequent expansion, (2) development of tendon-gel integrated bioprinting (TIP) technology for the fabrication of pre-cell fibers and subsequent differentiation to skeletal muscle, adipose, and blood capillary fibers, (3) assembly of the differentiated cell fibers to construct engineered steak-like meat by mimicking the histological structures of actual beef steak (Fig. 1b). Since tendon is a key tissue for anisotropic alignment and maturation of muscle fibers, we fabricated tendon gels by TIP for consecutive connection between muscle cell fibers and tendon gels to obtain scalable anisotropically aligned matured muscle fibers. In this study, a total of 72 fibers comprising 42 muscle, 28 adipose, and 2 blood capillary were constructed by TIP and subsequently assembled to fabricate a steak-like meat with a diameter of 5 mm and a length of 10 mm by

consulting histological images of actual Wagyu beef steak. TIP is expected to become a powerful technology for constructing engineered steak-like meat with desired location, component ratio, and amount of the three types of fibers.

Results and Discussion

Verification of Differentiation Conditions in Extracted bSCs and bADSCs

The bSCs were isolated from the masseter muscle of a 27-month-old Japanese black cow obtained from a slaughterhouse using a method modified from a previously reported one[7]. The crude cell fraction separated from the approved beef meat by collagenase treatment was cultured until passage (P) 3 for cell sorting. The $CD31^-$, $CD45^-$, $CD56^+$, and $CD29^+$ cells were isolated by FACS, in which $Pax7^+$ bSCs were around 80%. 2D culture of the isolated bSCs was performed to evaluate the capability of proliferation and differentiation into muscle cells with prolonged passaging. After seeding the bSCs the passage was counted after every 2 days of culture. The media for proliferation contains not only fetal bovine serum (FBS) and basic fibroblast growth factor but also a p38 inhibitor to maintain the differentiation capacity of proliferating bSCs[7]. The number of seeded bSCs doubled around once a day until P8, and around once every 2 days thereafter (Fig. 2a). The differentiation after 2 days of seeding was induced by changing the basic media to a differentiation media containing 2% horse serum (HS), which is a well-known differentiation induction method for muscle cells. The cells were immunostained with the antibody of myosin II heavy chain (MHC) after 5 days of differentiation induction. We quantified the differentiation capacity on passage number of the seeded bSCs by calculating the ratio of DAPI fluorescence intensity between MHC^+ and MHC^- cells from fluorescence images (Supplementary Fig. 1). The bSCs from P3 to P7 expressed a comparable differentiation level, but the differentiation capability of bSCs above P8

significantly decreased (Figs. 2b and 2c). Therefore, we conducted experiments using cells prior to P8.

Next, 3D encapsulated culture in collagen microfibers (CMF)/fibrin gel was performed for assessment of the adipogenic differentiation potential of bADSCs with a variety of media condition since it is known that the adipogenesis of adipose-derived stem cells (ADSCs) in 3D culture is higher than in 2D culture[25] and suitable differentiation factors rely on species[26]. Conventional human adipogenic factors like insulin, rosiglitazone, or troglitazone were thus first found with limited adipogenic induction potential (Supplementary Fig. 4), leading to the direct addition of free fatty acids (pristanic acid, phytanic acid, erucic acid, elaidic acid, oleic acid, palmitoleic acid, and myristoleic acid) to the culture medium[27]. The different combinations of the seven aforementioned free fatty acids were thus compared and the results showed significantly higher adipogenesis by lipids storage in vesicles in the cytoplasm of the bovine preadipocytes for all seven free fatty acids contained media (from 1.8 to 2.7 times more at day 13 of differentiation) (Fig. 2d and Supplementary Figs. 2 and 3). To further increase the lipogenesis until reaching a matured bovine adipocyte state, the transforming growth factor (TGF) type I receptor activin-like kinase 5 inhibitor (ALK5i) effect was evaluated because this factor is an inhibitor of the TGF-β receptor ALK5 and TGF-β family ligands, contained in the 10% FBS of the culture medium, which are known to inhibit both adipogenesis and adipocyte hypertrophy[28]. The TGF-β family also includes myostatin, which is expressed by the myocytes to impair adipogenesis[29]. In the context of future co-culture between bovine myoblasts and adipocytes, ALK5i appeared relevant for further inducing the adipogenic potential of the culture medium containing the seven free fatty acids. Several concentrations were thus assessed from 1 to 10 µM. The results showed a tendency to a higher lipogenesis by lipids storage with 5 µM ALK5i (Fig. 2e). The adipogenic maturation of the bADSCs then increased progressively between 3 and 7 days of differentiation (Fig. 2f).

Recently, ADSCs have been considered to be a useful cell source for angiogenesis in tissue engineering, but unlike human ADSCs there are no reports on endothelial differentiation of bADSCs[30,31]. Knowing that they lose their differentiation potentials during ADSCs culture expansion[32], bADSCs were thus used at P1 to evaluate their endothelial differentiation in the different conditions. HS was surprisingly found to be a significant inducer of its endothelial differentiation, even at low concentration (6.4 and 10 times more for 1 and 10% HS, compared to the 10% FBS condition), independently of the medium used, DMEM or F12K (Figs. 2g-h and Supplementary Fig. 5). Human serum also provided an enhanced endothelial differentiation, compared to the FBS condition, but was impaired by the low cell proliferation observed (Supplementary Fig. 5). The DMEM + 10% HS was then used for the endothelial differentiation from bADSCs in this study.

Bovine Muscle Fiber Fabrication by SBP

To organize the isolated bSCs into a cell fiber, we utilized an SBP in which a bioink is dispensed inside a supporting bath that is usually composed of hydrogel particles (or high-viscous polymer melt) with thixotropy. Several studies have demonstrated its promise in cell printing for structural controllability and stable printing during prolonged operation[18,19,21,22]. We selected gelatin and gellan gum as supporting bath materials, respectively, due to their edible, removable, and cell compatible properties. Gelatin is a gel at room temperature (RT) and a solution at 37°C, therefore it is easy to remove after printing by incubation at 37°C[17]. Gellan gum hydrogel is also known to dissolve in Tris-HCl buffer at pH 7.4 and at 37°C[33]. The gellan gum and gelatin were fabricated in bulk hydrogel and homogenized into granular particles for implementation in a supporting bath, and their thixotropy was confirmed (Supplementary Fig. 6). Firstly, we tried to print the bioink containing bSCs, fibrinogen, and Matrigel solution in media into the supporting bath mixed with granular particles of gelatin (G-

Gel) or gellan gum (G-GG) and thrombin for the fabrication of a fibrous muscle fiber mimicking the bundle of muscle fiber in steak (Supplementary Movies 1 and 2). With the confirmation of the gel formation followed by the removal of supporting baths, high cell viability was observed for 3 days after printing in both the G-Gel and G-GG by live/dead staining (Figs. 3a, 3b and Supplementary Fig. 7).

When the printed cell fiber was cultured in suspension, it transformed from a fibrous to a globular form (Fig. 3c). Studies related to muscle tissue engineering have implied that an anchor structure enables 3D muscle tissue to not only maintain its initial shape but also improve the cell alignment, fusion, and differentiation against the muscle fiber's contraction[15,34–38]. We placed a printed cell fiber onto a silicone rubber and anchored it with needles to fasten both ends to withstand cell contractions (Fig. 3d, left). With the needle fixed culture, the cell fibers printed inside G-GG and G-Gel retained the fibrous structure, but the diameter had shrunk by around 60% in G-GG and 80% in G-Gel at day 9 of culture (Fig. 3d, right). It would be reasonable to suppose that the size decrease was caused by alignment and fusion of bSCs with an enzymatic decomposition of fibrin gel by proteases secreted from cells[39,40]. We also took immunofluorescence images inside the cell fibers to examine the cellular behavior w/ and w/o needle anchoring after 7 days of differentiation. To quantify the improvement in terms of muscle maturation, the cell alignment, i.e. the angle setting for the straight line between needles, was measured from the immunofluorescence images (Fig 3e, left). The results showed that the cells in the cell fiber of suspension culture randomly oriented regardless of the type of supporting baths and in needle fixed culture the cells in the cell fiber printed inside G-Gel were highly anisotropically oriented compared to those of G-GG (Fig 3e, right). We postulate that the difference in the degree of alignment between G-GG and G-Gel arises from the hindrance of cell behaviors by residual substances that might exist inside or on the printed cell fibers. That is, the residual G-GG in the cell fiber may not be degraded or dissolved, in which case the

cells rarely remodel the ECM around them and are not able to migrate to fuse other cells (Supplementary Fig. 8). On the other hand, G-Gel is easily dissolved at 37℃ and may be degraded by proteases, enabling active cell behavior although there are residues inside the printed cell fiber. Printing bSCs inside G-Gel and anchoring them are essential steps for fabrication of the muscle cell fiber, but the anchoring method may not be appropriate for scale-up. Therefore, we developed a modified SBP to include a part to simultaneously anchor the printed cell fiber.

Fabrication of Muscle, Fat, and Vascular Cell Fibers by TIP

The important feature in the modified SBP, which we have named TIP, is the introduction of tendon-gels to anchor the printed cell fibers for culture. Fig. 4a illustrates the process of the TIP in which the printing bath is divided into three parts; bottom tendon-gel, supporting bath, and upper tendon-gel. G-Gel is used as a supporting bath as described in the above section and the volume of tendon-gels is filled with 4 wt% collagen nanofiber solution (CNFs) which shows the reversible sol-gel transition from 4℃ to 37℃ (Supplementary Fig. 9). To separate the layers and maintain the structure we fabricated polydimethylsiloxane (PDMS) wells (Supplementary Fig. 10). After bSCs fiber formation inside the PDMS well (Supplementary Movie 3), incubation for 2 h at 37℃ induced the supporting bath and tendon-gels to become a solution and gel, respectively, followed by placement of a PDMS well itself in the media for culture.

On day 3, we could confirm that the printed cell fiber maintained its fibrous shape with reduced size (data not shown) and that there was a connection between two tendon-gels in phase contrast and H&E staining images (Figs. 4b and 4c). The bSCs fiber by TIP also showed a high alignment of cells after 3 days of differentiation, which is comparable with that of the

needle fixed culture (Figs. 4d and 4e and Supplementary Movie 4). Interestingly, the sarcomere structure of matured muscle fibers was shown in some of the TIP derived bSCs fibers (Fig. 4f), but we could not show any cell fibers by the needle fixed culture after 14 day of differentiation. Even though we did not investigate thoroughly here, it may have been caused by cell adhesion of bSCs to the collagen gel at anchorage regions in the TIP whereas there is no cell adhesion in the needle fixed culture (Supplementary Fig. 11). TIP is a promising method for muscle fiber fabrication, but it still has a problem in that the bSCs fiber become detached from the tendon-gels, especially the bottom tendon-gels, in a prolonged culture due to its strong contraction. Increasing concentration of CNFs or additional crosslinking will hopefully provide a solution to this problem. Moreover, double printing, after fabrication of a cell fiber by general TIP, then rotating the PDMS well 180° so that it reversed and then printing one more time around the first formed cell fiber, may be another way of solving the problem. When double printing, two printed cell fibers close to each other are fused into one thicker cell fiber (Supplementary Fig. 13) and it seems to be more resilient to strong contraction than by simply printing once (data are not shown).

Multiple printing for 25 bSCs cell fiber fabrication in one large PDMS well was also performed, demonstrating the possibility of mass production of TIP (Fig. 4g and Supplementary Movie 5). We expected that large tissue composed of various types of cell fibers could be fabricated in one PDMS well, but we fabricated muscle, fat, and vascular cell fibers individually in this study because the differentiation should be induced in the media corresponding to each cell fiber based on the information discussed in the first section. After the success in optimization of the differentiated media for all three types of cell fibers at the same time, programed printing of them in desired locations will be feasible. Fig. 4g and Supplementary Movies 6-8 show whole muscle, adipose, and blood capillary cell fibers independently fabricated by TIP. Fat and vascular fibers were obtained by inducing the

adipogenesis of bADSCs fiber for 7 days and by culturing the cell fiber of endothelial-differentiated bADSCs for 7 days, respectively. The adipose fibers showed a high density of bovine adipocytes in a mature state, displaying a cytoplasm full of lipids vesicles. The blood capillary fibers were fully covered by CD31 expressing differentiated bovine endothelial cells (Fig. 4h and Supplementary Fig. 12).

The characteristics of cell concentration, compressive modulus, and water contents of muscle and adipose cell fibers by TIP were compared with the fibers extracted from commercial beef. Cell concentration of muscle and fat cell fibers of commercial beef were calculated from the DNA content of one tissue with a similar volume to TIP-derived cell fibers (Supplementary Fig. 14). While the cell density of the TIP-derived muscle and fat cell fibers were calculated to be $3x10^6$ and $3x10^5$ cells/fiber, respectively, the cell densities of muscle and fat cell fibers of commercial beef were $8.61x10^5$ and $1.89x10^5$ cells/fiber (Fig. 4i). The reason for the approximately fourfold higher cell density of TIP muscle fibers seems to be lower maturation (fusion) of differentiated satellite cells because higher maturation induces lower cell numbers because of cell fusion. Although water content showed the disparity between commercial beef and TIP-derived cell fibers (Supplementary Fig. 16), the compressive modulus in all cell fibers showed a similar value, which was within one order of kPa (Fig. 4j and Supplementary Fig. 15). Since the TIP-derived cell fibers were not controlled for tenderness, flavor, and additional nutrient components in this study, these factors will need to be addressed to produce customer-oriented cultured meat.

Engineered Steak Construction by Assembly of Muscle, Fat, and Vascular Cell Fibers

The assembly of TIP-derived cell fibers was attempted to demonstrate the construction of cultured steak. To mimic the structure of commercial beef, we first took a cross-sectional image

of Wagyu by sarcomeric α-actinin and laminin staining, which denote muscle in double-positive and adipose in laminin only positive, respectively (Fig. 5a, left). We tried to produce cultured steak with dimensions of approximately 5 mm x 10 mm x 5 mm (WxLxH), and from Wagyu's image we made the model image showing the required number of muscle, adipose, and blood capillary cell fibers and arrangement (Fig. 5a, right). The diameters of the cell fibers obtained by TIP were estimated to be approximately 500, 760, and 600 μm, which means the required number of each cell fiber were 42, 28, and 2, respectively. To distinguish each cell fiber, muscle and vascular cell fibers were stained in red using food coloring, leaving fat cell fiber as a white color. After physically stacking the cell fibers like the model image, it was treated with transglutaminase which is a common food crosslinking enzyme to accelerate the assembly for 2 days at 4°C. The final product is shown in Fig. 5b and the cross-sectional image was taken to verify that the structure was analogous to Wagyu (Fig. 5c). which implied the feasibility of TIP-based engineered steak fabrication.

Conclusion

In this research, we reported a new technology for constructing cultured steak-like meat with muscle, adipose, and blood capillary cell fibers composed of edible bovine cells. After isolation and purification of bSCs and bADSCs, we verified cell behaviors; the proliferation and differentiation of bSCs and adipogenesis and vasculogenesis from bADSCs depending on media conditions. It was shown that resistance to the contraction force during culture of bSCs derived cell fiber was essential to realize highly aligned muscle fibrils. A modified supporting bath assisted cell printing method, TIP, was developed, in which the collagen gel-based tendon tissues withstands cell traction force during bSCs differentiation, leading to a well-maintained fibrous structure and anisotropic cell alignment during bSCs differentiation. Comparison of

cell density, compressive modulus, and water content showed the gap between TIP derived and commercial muscle and fat cell fibers. Further elaboration will therefore be required with consideration of texture and flavor in future. We demonstrated engineered meat analogous to the structure of commercial beef through the assembly of muscle, adipose, and blood capillary cell fibers due to TIP's multiple cell fiber printing, which could be beneficial for the scale-up of not only cultured meat but also muscle tissue engineering in the future.

Methods

Isolation and purification of bSCs and bADSCs. bSC were isolated from 160 g fresh masseter muscle samples (within 6 h of euthanasia) of 27-month-old Japanese black cattle obtained at a slaughterhouse as previously described[7] with some modifications. The freshly harvested bovine muscle was kept on ice, transferred to a clean bench, and washed with cold 70% ethanol for 1 min, followed by cold PBS1x 2 times. Then, the fat tissues were removed, cut into small pieces with a knife, and minced with a food processor mechanically. The bovine minced muscle was washed with cold PBS1x with 1% penicillin-streptomycin (P.S.) (Lonza, 17-745E) for 1 min. The washed muscle was transferred to a bottle and mixed with 160 ml of 0.2% collagenase II (Worthington, CLS-2) in DMEM (Invitrogen, 41966-29) supplemented with 1% P.S.. After digestion, 160 ml 20% FBS in DMEM supplemented with 1% P.S. was added and mixed well. The mixed solution was centrifuged for 3 min at 80 g and 4 °C. Floating tissues in the supernatant after centrifugation was removed by tweezers and then collected supernatant kept on ice as a mononuclear cell suspension. Precipitated debris was mixed with 80 ml cold 1% P.S. in PBS1x and centrifuged for 3 min at 80 g and 4 °C. The supernatant was collected again and mixed with the former mononuclear cell suspension. After that, the cells were filtered through a 100 µm cell strainer. After centrifugation for 5 min at 1,500 g and 4 °C, the cells were suspended with 160 ml cold DMEM with 20% FBS and 1% P.S., were filtered through a 100 µm cell strainer followed by a 40 µm cell strainer. The cells were then centrifuged for 5 min at 1,500 g and 4 °C. Precipitated cells were incubated with 8 ml erythrocyte lysis buffer (ACK, 786-650) for 5 min on ice. Then the cells were washed twice with cold PBS1x supplemented with 1% P.S. and the cell pellet was mixed with FBS supplement with 10% dimethyl sulfoxide and then reserved at -150 °C. The frozen cells were recovered in a 37 °C water bath and washed with cold PBS1x twice. The cells were suspended in F10 medium (Gibco, 31550-023) containing 20% FBS, 5 ng/mL bFGF (R&D, 233-FB-025) and 1% P.S. supplemented with 10µM p38i (Selleck, S1076), and then seeded at $1.1x10^5$ cells/well in 6-well cell culture plates (Corning) that were coated with 0.05% bovine collagen type I (Sigma, C4243). The cells were cultured by changing the medium every two or three days and then passage the cells when they reach 60% of confluency until passage 3 for cell sorting by flow cytometry. The cells were suspended in FACS buffer (1% BSA in PBS1x) and stained with APC anti-human CD29 Antibody (BioLegend, 303008), PE-Cy^{TM7} anti-human CD56 (BD, 335826), FITC anti-sheep CD31 (BIO-RAD, MCA1097F), FITC anti-sheep CD45 (BIO-RAD, MCA2220F) for 30–45 min on ice under dark. After antibody incubation, the cells were washed twice with cold PBS1x and reconstituted in PBS1x with 2% FBS. The $CD31^-CD45^-CD56^+CD29^+$ cells were isolated by Sony Cell Sorter SH800S as bSCs.

Subcutaneous and kidney bovine adipose tissues were isolated at slaughter house on the day of slaughter and send to the laboratory with a ice pack. Following the 24h duration delivery. The tissues were first washed in PBS1x containing 5% of penicillin-streptomycin-amphotericin B (Wako, 161-23181). Then, 8-10 g of tissue was separated into fragments to fill the 6 wells of a 6-well plate and were minced to get around $1mm^3$ in size using autoclaved scissors and tweeters, directly in 2 mL of collagenase solution containing both collagenase type I (Sigma Aldrich, C0130) and type II (Sigma Aldrich, C6885) at 2 mg/mL for each in DMEM with 0% FBS, 5% BSA and 1% antibodies (sterilized by 0.2µm filtration). After one hour of incubation at 37ºC with 250 rpm agitation, DMEM (Nacalai, 08458-16) was added and the lysate was filtrated using a sterilized 500 µm iron mesh filter, before being centrifuged 3 min at 80 g. The upper human mature adipocytes layer was then removed and the pellet containing the stromal vascular fraction (SVF) was washed two times in PBS1x with 5% BSA and 1% antibiotics and once in complete DMEM, by 3 min of centrifugation at 80 g between each wash. Finally, the pellet containing the SVF cells was resuspended in DMEM and seeded in a 10 cm dish for expansion by changing the medium every day for three days and then passage the cells when they reach 80% of confluency. After P1, the remaining adherent cells are considered as bADSCs and were expanded in DMEM.

2D cell culture. bSCs were cultured in high-glucose DMEM (Gibco, 10569-010) containing 1% antibiotic-antimycotic mixed solution (Nacalai, 02892-54), 10% FBS, 4 ng/mL fibroblast growth factor (Fujifilm, 067-04031), and 10 uM p38 inhibitor (Selleck, SB203580) for proliferation and bSCs within P8 were used for all experiments. For differentiation induction of bSCs, the media changed to DMEM containing 2% horse serum and 1% antibiotic-antimycotic mixed solution. To investigate the cell proliferation and differentiation ratio 50,000 cells were seeded on 24 well plates, and differentiation media was replaced every 2 days after differentiation induction.

Culture and differentiation of bADSCs to bovine endothelial cells. To monitor the endothelial differentiation of bADSCs, bADSCs at P1 previously expanded in DMEM were seeded at 5,000 cells on 48 well plates, and kept 7 days in different conditions (DMEM with 10% FBS, HS, human serum or calf serum, F12K medium with 10% HS or DMEM with 1 or 5% HS), by renewing media every 2-3 days.

Collagen microfibers preparation. Based on our previous study[41], the collagen microfibers (CMF) were first prepared from a collagen type I sponge after dehydration condensation at 200°C for 24 h crosslinking. The crosslinked collagen sponge was mixed with ultra-pure water at a concentration of 10 mg/mL (pH=7.4, 25°C) and homogenized for 6 min at 30,000 rpm. Then, the solution was ultrasonicated (Ultrasonic processor VC50, SONICS) in an ice bath for 100 cycles (1 cycle comprised 20 s ultrasonication and 10 s cooling) and filtrated (40 µm filter, microsyringe 25 mm filter holder, Merck), before being freeze-dried for 48 h (FDU-2200, EYELA). The obtained CMF was kept in a desiccator at RT.

3D gel embedded culture. To construct the 3D drops adipose tissues, CMF were first weighted and washed in DMEM without FBS by being centrifuged 1 min at 10,000 rpm to get a final concentration in the tissues of 1.2 wt%. The bADSCs were added after trypsin detachment (always used at P1-3) and centrifuged 1 min at 3,500 rpm to get a final cell concentration of $5x10^6$ cells/mL. The pellet containing CMF and bADSCs was then mixed in a fibrinogen (Sigma Aldrich, F8630) solution at 6 mg/mL final concentration (the stock solution at 50 mg/mL prepared in DMEM with 10% FBS & 1% antibiotics) and the thrombin solution (Sigma Aldrich, T4648) was added to get a final concentration of 3 U/mL (the stock solution at 50 U/mL prepared in DMEM with 10% FBS & 1% antibiotics). Finally, 2 µL drop tissues were seeded in a 96 well plate (Iwaki, 3860-096) and gelated during 15 min in the incubator at 37°C. Then 300 µL of medium was added on the drops tissues. For adipogenic differentiation, 3 days of proliferation were first necessary for proliferation and cell-cell contacts. The medium was then switched for DMEM with 10% FBS containing different adipogenic components to compare: Rosiglitazone (at 20 µM final concentration, Sigma Aldrich, R2408), Insulin (at 10 µg/mL final concentration, Sigma Aldrich, I6634), Troglitazone (at 40µM final concentration, Sigma Aldrich, T2573), Pristanic acid (at 50 µM final concentration, Funakoshi, 11-1500), Phytanic acid (at 50 µM final concentration, Sigma Aldrich, P4060), Erucic acid (at 50 µM final concentration, Sigma Aldrich, 45629-F), Elaidic acid (at 50 µM final concentration, Sigma Aldrich, 45089), Oleic acid (at 50µM final concentration, Sigma Aldrich, O1383), Palmitoleic acid (at 50 µM final concentration, Sigma Aldrich, 76169), Myristoleic acid (at 50 µM final concentration, Sigma Aldrich, 41788), TGF type I receptor activin-like kinase 5 inhibitor (ALK5i II, 2-[3-(6-methyl-2-pyridinyl)-1H-pyrazol-4-yl]-1,5-naphthyridine, at 1-10 µM final concentration, Cayman, 14794) or Bovine Endothelial Cell Growth Medium (Cell Applications Inc., B211K-500). The 300 µL of differentiation medium was then renewed every 2-3 days until 13 days of differentiation.

SBP & culture. G-GG was produced by preparing a 1 wt% gellan gum (Sansho) in PBS1x, grinding it with a homogenizer, centrifuging at 4200 rpm for 3 min, and removing the supernatant. G-Gel was produced by preparing of 4.5 wt% porcine gelatin (Sigma Aldrich, G1890) in DMEM containing 1% antibiotic-antimycotic mixed solution and 10% FBS, putting it at 4°C overnight for gelation, adding the same volume of DMEM to the gelatin gel, grinding it with a homogenizer, centrifuging at 4200 rpm for 3 min, and removing the supernatant. The bioink was prepared to be $5x10^7$ cells/mL of bSCs in the mixture composed of 20 mg/mL fibrinogen (Sigma Aldrich, F8630) in DMEM and Matrigel (Corning, 356234) (6:4, v/v). The supporting bath was prepared by mixing G-GG or G-Gel with 10 U/mL thrombin (Sigma Aldrich, T4648) before printing. After filling the prepared supporting bath in a glass vial and loading the syringe containing the prepared bioink onto the dispenser instrument (Musashi, Shotmaster 200DS), cell printing was conducted inside the supporting bath maintaining the syringe and bed parts of the instrument at 4°C. All parts, such as syringes, nozzles, and containers used for cell printing, were sterilized with 70% ethanol and UV treatment. The nozzle gauge, moving speed, and dispensing speed was 16G, 1 mm/s, and 23sp (sp is the speed unit defined in the equipment), respectively. The printed structures inside the supporting baths were incubated inside a sterile cabinet at RT for 1 h to ensure gelation. After gelation, the G-GG was gently removed by pipetting and was immersed in 50 mM Tris-HCl buffer (pH 7.4) at 37°C for 30 min, and repeat the same process one more time. G-Gel was dissolved by incubation at 37°C for 2 h. The obtained cell fibers after removal of supporting baths were cultured in the basic media of bSCs for 2-3 days and then replaced with differentiation media. Suspension culture was simply conducted by placing the printed cell fiber on a tissue culture plate, and needle fixed culture was conducted by fixing both ends of the printed cell fibers onto the silicone rubber with a size of 2 cm x 2 cm x 3 mm (WxDxH) placed on a 6 well plate.

PDMS well fabrication. The parts of PLA molds were fabricated by the FDM 3D printer (Creality, Ender-3) after modeling by Fusion360 and slicing by Cura for PDMS wells. PDMS (Corning, Sylgard 184) was poured into the assembled PLA mold and cured at 50°C overnight, the PDMS wells were obtained by removal of PLA molds.

TIP & culture. 4 wt% CNFs was produced from collagen sponge (Nipponham, Type I & III mixture) based on the previous method. After cutting a small area of PDMS wells' side to make the media flow channel, it was sterilized with 70% ethanol and UV treatment, then put it on the slide glass. The PDMS well was filled with 4 wt% CNFs, G-Gel, and 4 wt% CNFs at the bottom, middle, and top layers, respectively. Cell printing was conducted the same as that of SBP. After printing cells, printed area at the top layer of PDMS well was covered one more time with 4 wt% CNFs, incubated at RT for 1 h, and then it was incubated at 37°C for 2 h to dissolves G-Gel and induce CNFs gelation, and finally placed in a culture container. The bioinks were prepared the same as in SBP for muscle cell fiber, by mixing $5x10^6$ cells/mL of bADSCs in 1.2 wt% CMF and 20 mg/mL Fibrinogen solution for fat fibers and $10x10^6$ cells/mL of endothelial differentiated bADSCs in 1.2 wt% CMF and 20 mg/mL Fibrinogen solution for vascular fibers.

Live/dead staining. Printed cell fibers were stained with 2 µM calcein-AM and 4 µM ethidium homodimer-1 (Invitrogen, L3224) in DMEM at 37°C for 15 min followed by rinsing with PBS1x and fluorescence imaging by confocal microscopy (Olympus, FV3000). From fluorescence images, % cell viability was calculated by live cells divided by dead cells.

Histological staining. Tissues were washed once in PBS1x and then fixed in 4% paraformaldehyde (Wako, 163-20145) overnight at 4°C followed by three times washes in PBS1x. The samples were then maintained in PBS1x solution before being mounted in paraffin-embedded blocks. Paraffin-embedded blocks and sections were prepared and hematoxylin/eosin (H/E) stained by the Applied Medical Research Laboratory, Inc. Some pieces of commercial (Wagyu) beef steak were immersed in 4% paraformaldehyde solution overnight at 4 ºC, and then in 1/15M phosphate buffer (pH 7.4) containing 30% sucrose. They were rapidly frozen in dry ice acetone and cut into 20 µm thick sections. The tissue sections were processed for immunostaining for sarcomeric alpha-actinin and laminin to depict myotubes of skeletal muscles and basement membranes of the muscles and adipose tissues. The immunostaing was performed by use of specific antibodies against sarcomeric alpha actinin (abcam, EA 63) and laminin (Sigma-Aldrich, L9393), and the reaction products were visualized in blue (Vector Laboratories, Vector Blue) and brown (DAKO, DAB+ chromogen), respectively.

Immunostaining. Immunostaining was conducted by a general process, 4% paraformaldehyde fixation at RT for 15 min or at 4°C overnight, permeabilization with 0.2% Triton X-100 (Sigma Aldrich, T8787) at RT for 15 min, blocking with 1% BSA (Sigma-Aldrich, A3294) for 30 min, incubation with 1st antibody in 1% BSA at RT for 2 h or at 4°C overnight, incubated with cocktails containing fluorophore conjugated 2nd antibody and 1 µg/mL TRICT-phalloidin (Sigma Aldrich, P-1951) for actin staining or 100 ng/mL NileRed (TCI, N0659) for lipid staining at RT for 1 h, finally 300 nM DAPI (Invitrogen, D21490) counterstaining. Myosin 4 Monoclonal Antibody (eBioscience, 14-6503-82) for bSCs and Anti-CD31 (Wako, M0823) for bovine endothelial cells were used as 1st antibodies. Goat anti-Mouse IgG (H+L) Cross-Adsorbed Secondary Antibody, Alexa Fluor 488 (Invitrogen, A-11001) and goat anti-Mouse IgG (H+L) Cross-Adsorbed Secondary Antibody, Alexa Fluor 647 (Invitrogen, A-21235) were used as 2nd antibodies. All fluorescence images were taken by confocal microscopy. In the case of printed cell fibers, Rapiclear 1.52 (SUNJin Lab) was treated at RT for 30 min for deep tissue imaging.

Rheology measurement. Viscosity was measured by the controlled rate mode of rheometer (Thermo Scientific, HAAKE RheoStress 6000) to verify the thixotropy of G-Gel and G-GG. The steps were composed of at 0.01/s for 30 s, at 30/s for 100 s, and at 0.01/s for 30 s.

UV-Vis. The disposable cuvette was filling with 1 mL of 4wt% CNFs, and then transmittance was measured at the temperature-controlled steps by UV-Vis spectrometer (Jasco, V-670); at 4°C for 2000 s, at 37°C for 2000 s, at 4°C for 2000 s, and then at 37°C for 2000 s. After each temperature change, the photos of the samples were taken.

Mechanical test. The elastic modulus of this printed fibers was measured with EZ test (SHIMADZU, EZ/CE 500N). After preparing the different printed fibers, they were kept in a 24-well Transwell insert at RT for measuring. A spherical mold (5 mm in diameter) was used to measure elastic modulus at a head moving speed of 1.0 mm/min. The compressive test protocol was employed increasing the engineering strain until the testing stress to 200 mN. The modulus is automatically calculated by EZ test in elastic range (10-20 mN).

Water content measurement. The water content is calculated according to the mass before and after freeze drying. Briefly, the printed fibers in PBS1x was taken out, the surface liquid was removed, and the wet weight (W_{wet}) of the fibers was measured by a balance. The dry weight (W_{dry}) of the fibers was measured after freeze drying (24 h). The water content is given by the following formula:

$$V_{water} = \frac{W_{wet} - W_{dry}}{W_{wet}} \times 100$$

DNA content measurement. Commercial beef was bought from supermarket and intramuscular fat tissues as wells as muscle tissues parts were cut in small fibers of the same size than the printed fibers (Fig. S12). One fiber was put per microcentrifuge tube and the tissues were lysed following the DNeasy Blood & Tissue Kit (QIAGEN, 69504) to extract their DNA content, which was quantified by the NanodropTM N1000 device (Thermo Fisher Scientific). Then to estimate the cell number from the DNA amount, it was considered that one mammalian cell contains around 6 pg of DNA[42], which allows the evaluation of the total cell number per fiber.

Image processing & analysis. For the evaluation of bSCs differentiation on 2D culture, at least 4 the fluorescence images of the samples stained with DAPI and MF20 were taken in size of about 6 mm x 6 mm, and the number of nuclei in all areas and MHC positive area was measured by ImageJ. For calculation of adipogenesis ratio from bADSCs, NileRed lipids total fluorescence intensity, as well as Hoechst nuclei, total fluorescent intensity per picture were measured from greyscale images using ImageJ software and the ratios were compared. For vasculogenesis ratio from bADSCs, the same method was applied, using CD31's total fluorescence intensity normalized by Hoechst total fluorescence intensity ratios. 3D reconstructed image and the printed cell fibers' 3D movie was obtained by Imaris software (Bitplane).

Figure legends

Fig. 1 Overview of work a, Structure of steak. (i-ii) H&E- and (iii) Azan-stained images of a piece of steak. All scale bar denotes 100 μm (iv) Schematic of hierarchical structure in muscle. b, Schematic of the construction process for cultured steak. The first step is cell purification of tissue from cattle to obtain bovine satellite cells (bSCs) and bovine adipose-derived stem cells (bADSCs). Second is supporting bath assisted printing (SBP) of bSCs and bADSCs to fabricate the muscle, fat, and vascular tissue with a fibrous structure. The third is the assembly of cell fibers to mimic the commercial steak's structure. *SVF: stromal vascular fraction

Fig. 2 Verification of purified bovine stem cells. a-b, Proliferation rate **(a)** and differentiation ratio on day 5 of differentiation **(b)** of bSCs from passage 3 (P3) to P12 cultured on a tissue culture plate. Red line and blue line are a slope from P3 to P8 and from P8 to P12, respectively. **c**, Representative fluorescence images of differentiation induced bSCs at P7 and P9 stained for myosin II heavy chain (MHC) (green) and nucleus (blue). Scale bars, 1 mm. **d**, Adipogenesis ratio (left) of 3D gel drop cultured bADSCs derived by 12 combinations of free fatty acids (middle) in DMEM on day 3, 9, and 13 and representative fluorescence images (right) of differentiation induced bADSCs by #1 and #12 combinations of fatty acid on day 13 (red: lipid & blue: nucleus). Statistical significance was calculated with 2-ways ANOVA with Tukey multiple comparison test, n=12 drops tissues/per condition and 2 pictures per drop. Scale bars, 100 μm. **e-f**, Adipogenesis ratio (left) and representative fluorescence images (right) of 3D gel drop cultured bADSCs depending on the concentration of ALK5i on day 7 **(e)** and culture day **(f)** in the #1 combination of free fatty acids (red: lipid & blue: nucleus). Statistical significance was calculated with 1-way ANOVA with Tukey multiple comparison tests, n=2-3 drops tissues/per condition. Scale bars, 100 μm. **g-h**, Vasculogenesis ratio of bADSCs depending on serum conditions in DMEM **(g)** and base media **(h)** on day 7 (magenta: CD31 & blue: nucleus). Statistical significance was calculated with 1-way ANOVA with Tukey multiple comparison test, n=3 different wells/condition, 3 pictures/well. **i**, Representative fluorescence images of bADSCs depending on serum conditions on day 7 stained for CD31 (magenta) and nucleus (blue). Scale bars, 1 mm. The used bADSCs were extracted from subcutaneous fat. *P<0.05, **P<0.01, ***P<0.001; error bars represent mean ± s.d.

Fig. 3 The characterization of bSCs tissue fabricated by SBP. a-b, Optical (left), phase contrast (middle), and fluorescence (right, green: live cells & red: dead cells) images of the bSCs tissues printed inside granular gellan gum (G-GG) **(a)** and granular gelatin (G-Gel) **(b)** followed by bath removal. Scale bars, 500 μm. **c**, Shape change of bSCs tissue fabricated by SBP inside G-Gel from the fibrous form right after printing and bath removal to globular form on day 6 of suspension culture. **d**, Schematic (left), size change in accordance with culture day (middle), and phase-contrast images (right) of needle fixed culture of printed bSCs tissues. Error bars represent mean ± s.d. Scale bars, 500 μm. **e**, Fluorescence images (upper, red: actin & green: MHC) and cell alignment measurements (lower) of the bSCs tissues printed inside G-GG and G-Gel and in suspension and needle fixed cultures on day 3 of differentiation, respectively. Scale bars, 200 μm.

Fig. 4 Tendon integrated bioprinting (TIP) for muscle, fat, vascular tissue fabrication. a, The schematic of TIP for cell printing. **b**, Optical (upper) and phase-contrast (lower) images of the bSCs tissue printed by TIP, keeping the fibrous structure on day 3. The images were taken after fixation. Scale bar, 1 mm. **c**, The H&E stained image of half of collagen gel (dotted black line) - fibrous bSCs tissue (dotted red line) and a magnified image of the fibrous bSCs tissue (right). Scale bars, 2 mm (left) and 50 μm (right). **d**, 3D fluorescence image (left) and cell alignment measurement (right) of the TIP-derived bSCs tissue stained with actin (red) and MHC (green) on 3 day of differentiation. Scale bar, 50 μm. **e**, SEM images of TIP-derived bSCs tissue on 3 day of differentiation. Scale bars, 10 μm & 100 μm (inset). **f**, Fluorescence image of TIP-derived bSCs tissue stained with actin (red), MHC (green), and nucleus (blue) on 14 day of differentiation. A scale bar, 50 μm. **g**, The optical images of multiple tissue fabrication (25 ea.) by large-scale TIP. **h**, Whole fluorescence (left), optical (inset), and magnified (right) images of muscle (on day 4 of differentiation, green: MHC & blue: nucleus), fat (on day 7 of differentiation, red: lipid & blue: nucleus), and vascular (on day 7, red: CD31 & blue: nucleus) tissues fabricated by TIP. Scale bars, 1 mm (left) and 100 μm (right). **i-j**, Cell concentrations (Calculated values in TIP-derived) **(i)** and compressive modulus **(j)** of muscle and fat fibers in the commercial meat and TIP-derived. Statistical significance was calculated with 1-way ANOVA with Tukey multiple comparison test. *$P<0.05$; error bars represent mean ± s.d.

Fig. 5 Assembly of fibrous muscle, fat, and vascular tissues to cultured steak. a, Assembly schematic (right) based sarcomeric α-actinin (blue) & laminin (brown) stained image (left) of the commercial meat (Wagyu). It is assumed that the diameter of the fibrous muscle, fat, and vascular tissues are about 500, 760, and 600 μm, respectively. Scale bar, 1 mm. **b-c**, Optical images of the cultured steak by assembling muscle (42 ea.), fat (28 ea.), and vascular (2 ea.) tissues at **(b)** top and **(c)** cross-section view of the dotted line area. Muscle and vascular tissue were stained with carmine (red color), but fat tissue was not.

References

1. Bhat, Z. F., Morton, J. D., Mason, S. L., Bekhit, A. E.-D. A. & Bhat, H. F. Technological, Regulatory, and Ethical Aspects of In Vitro Meat: A Future Slaughter-Free Harvest. *Comprehensive Reviews in Food Science and Food Safety* **18**, 1192–1208 (2019).
2. Chriki, S. & Hocquette, J.-F. The Myth of Cultured Meat: A Review. *Front Nutr* **7**, (2020).
3. Zhang, G. *et al.* Challenges and possibilities for bio-manufacturing cultured meat. *Trends in Food Science & Technology* **97**, 443–450 (2020).
4. Ben-Arye, T. *et al.* Textured soy protein scaffolds enable the generation of three-dimensional bovine skeletal muscle tissue for cell-based meat. *Nat Food* (2020) doi:10.1038/s43016-020-0046-5.
5. Bodiou, V., Moutsatsou, P. & Post, M. J. Microcarriers for Upscaling Cultured Meat Production. *Front. Nutr.* **7**, (2020).
6. Post, M. J. Cultured meat from stem cells: Challenges and prospects. *Meat Science* **92**, 297–301 (2012).
7. Ding, S. *et al.* Maintaining bovine satellite cells stemness through p38 pathway. *Scientific Reports* **8**, 10808 (2018).
8. Choudhury, D., Tseng, T. W. & Swartz, E. The Business of Cultured Meat. *Trends in Biotechnology* **38**, 573–577 (2020).
9. Post, M. J. *et al.* Scientific, sustainability and regulatory challenges of cultured meat. *Nat Food* **1**, 403–415 (2020).
10. Takahashi, H., Shimizu, T. & Okano, T. Engineered Human Contractile Myofiber Sheets as a Platform for Studies of Skeletal Muscle Physiology. *Scientific Reports* **8**, 13932 (2018).
11. Jiao, A. *et al.* Thermoresponsive Nanofabricated Substratum for the Engineering of Three-Dimensional Tissues with Layer-by-Layer Architectural Control. https://pubs.acs.org/doi/abs/10.1021/nn4063962 (2014) doi:10.1021/nn4063962.
12. Onoe, H. *et al.* Metre-long cell-laden microfibres exhibit tissue morphologies and functions. *Nature Mater* **12**, 584–590 (2013).
13. Kim, W., Kim, M. & Kim, G. H. 3D-Printed Biomimetic Scaffold Simulating Microfibril Muscle Structure. *Advanced Functional Materials* **28**, 1800405 (2018).
14. Costantini, M. *et al.* Microfluidic-enhanced 3D bioprinting of aligned myoblast-laden hydrogels leads to functionally organized myofibers in vitro and in vivo. *Biomaterials* **131**, 98–110 (2017).
15. Choi, Y.-J. *et al.* 3D Cell Printing of Functional Skeletal Muscle Constructs Using Skeletal Muscle-Derived Bioink. *Advanced Healthcare Materials* **5**, 2636–2645 (2016).
16. Bhattacharjee, T. *et al.* Writing in the granular gel medium. *Science Advances* **1**, e1500655 (2015).
17. Hinton, T. J. *et al.* Three-dimensional printing of complex biological structures by freeform reversible embedding of suspended hydrogels. *Science Advances* **1**, e1500758 (2015).
18. Choi, Y.-J. *et al.* A 3D cell printed muscle construct with tissue-derived bioink for the treatment of volumetric muscle loss. *Biomaterials* **206**, 160–169 (2019).
19. Jeon, O. *et al.* Individual cell-only bioink and photocurable supporting medium for 3D printing and generation of engineered tissues with complex geometries. *Mater. Horiz.* 10.1039.C9MH00375D (2019) doi:10.1039/C9MH00375D.
20. Lee, A. *et al.* 3D bioprinting of collagen to rebuild components of the human heart. *Science* **365**, 482–487 (2019).

21. Noor, N. *et al.* 3D Printing of Personalized Thick and Perfusable Cardiac Patches and Hearts. *Advanced Science* 1900344 (2019) doi:10.1002/advs.201900344.
22. Skylar-Scott, M. A. *et al.* Biomanufacturing of organ-specific tissues with high cellular density and embedded vascular channels. *Science Advances* **5**, eaaw2459 (2019).
23. Hena, S. A., Sonfada, M. L., Shehu, S. A. & Jibir, M. Determination of perimysial and fascicular diameters of triceps brachii, biceps brachii and deltoid muscles in Zebu cattle and one-humped camels. *Sokoto J. Vet. Sc.* **15**, 74 (2017).
24. Ministry of Education, Culture, Sports, Science and Technology. *Standards Tables of Food Composition in Japan (Seventh Revised Edition).* (2015).
25. Louis, F., Kitano, S., Mano, J. F. & Matsusaki, M. 3D collagen microfibers stimulate the functionality of preadipocytes and maintain the phenotype of mature adipocytes for long term cultures. *Acta Biomaterialia* **84**, 194–207 (2019).
26. Laliotis, G. P., Bizelis, I. & Rogdakis, E. Comparative Approach of the de novo Fatty Acid Synthesis (Lipogenesis) between Ruminant and Non Ruminant Mammalian Species: From Biochemical Level to the Main Regulatory Lipogenic Genes. *Curr Genomics* **11**, 168–183 (2010).
27. Mehta, F., Theunissen, R. & Post, M. J. Adipogenesis from Bovine Precursors. in *Myogenesis: Methods and Protocols* (ed. Rønning, S. B.) 111–125 (Springer, 2019). doi:10.1007/978-1-4939-8897-6_8.
28. Lee, M.-J. Transforming growth factor beta superfamily regulation of adipose tissue biology in obesity. *Biochimica et Biophysica Acta (BBA) - Molecular Basis of Disease* **1864**, 1160–1171 (2018).
29. Deng, B. *et al.* The function of myostatin in the regulation of fat mass in mammals. *Nutrition & Metabolism* **14**, 29 (2017).
30. Muller, S. *et al.* Human adipose stromal-vascular fraction self-organizes to form vascularized adipose tissue in 3D cultures. *Sci Rep* **9**, 7250 (2019).
31. Sarkanen, J.-R. *et al.* Adipose Stromal Cell Tubule Network Model Provides a Versatile Tool for Vascular Research and Tissue Engineering. *CTO* **196**, 385–397 (2012).
32. Zhu, Y. *et al.* Adipose-derived stem cell: a better stem cell than BMSC. *Cell Biochemistry and Function* **26**, 664–675 (2008).
33. Matsusaki, M. *et al.* Fabrication of Perfusable Pseudo Blood Vessels by Controlling Sol–Gel Transition of Gellan Gum Templates. *ACS Biomater. Sci. Eng.* acsbiomaterials.8b01272 (2019) doi:10.1021/acsbiomaterials.8b01272.
34. Morimoto, Y., Kato-Negishi, M., Onoe, H. & Takeuchi, S. Three-dimensional neuron–muscle constructs with neuromuscular junctions. *Biomaterials* **34**, 9413–9419 (2013).
35. Heher, P. *et al.* A novel bioreactor for the generation of highly aligned 3D skeletal muscle-like constructs through orientation of fibrin via application of static strain. *Acta Biomaterialia* **24**, 251–265 (2015).
36. Jones, J. M. *et al.* An Assessment of Myotube Morphology, Matrix Deformation, and Myogenic mRNA Expression in Custom-Built and Commercially Available Engineered Muscle Chamber Configurations. *Frontiers in Physiology* **9**, (2018).
37. Prüller, J., Mannhardt, I., Eschenhagen, T., Zammit, P. S. & Figeac, N. Satellite cells delivered in their niche efficiently generate functional myotubes in three-dimensional cell culture. *PLOS ONE* **13**, e0202574 (2018).
38. Rao, L., Qian, Y., Khodabukus, A., Ribar, T. & Bursac, N. Engineering human pluripotent stem cells into a functional skeletal muscle tissue. *Nature Communications* **9**, (2018).

39. Suelves, M. *et al.* Plasmin activity is required for myogenesis in vitro and skeletal muscle regeneration in vivo. *Blood* **99**, 2835–2844 (2002).
40. Guérin, C. W. & Holland, P. C. Synthesis and secretion of matrix-degrading metalloproteases by human skeletal muscle satellite cells. *Dev. Dyn.* **202**, 91–99 (1995).
41. Liu, H., Kitano, S., Irie, S., Levato, R. & Matsusaki, M. Capillary Alignment: Collagen Microfibers Induce Blood Capillary Orientation and Open Vascular Lumen (Adv. Biosys. 5/2020). *Advanced Biosystems* **4**, 2070052 (2020).
42. Gillooly, J. F., Hein, A. & Damiani, R. Nuclear DNA Content Varies with Cell Size across Human Cell Types. *Cold Spring Harb Perspect Biol* **7**, (2015).

Acknowledgements

We thank Yuko Fukushima from Kirin Holdings for bSCs preparation, Noboru Hiraoka for rheological measurements, and Prof. Sowa from Kyoto Prefecture University for an experimental design. The authors acknowledge financial support by Mirai-Program (18077228) from JST and Grant-in-Aid for Scientific Research (A) (20H00665) from JSPS.

Author Contributions

D.-H. K. and M.M. contributed to design the study and mainly draft the manuscript; D.-H. K., F.L., and H.L. carried out the cell culture, bioprinting experiments, biological analysis; F.L. and H.L. also contributed to draft the manuscript; H.S. conducted the histological experiment and analysis; Y.N., H.N., and M.K. provided practical advice and primary cultured bovine cells; D.T., D.K., S.I., and S.K., provided technical guidance and advice on bioprinting instruments; E.J. provided critical advice on muscle biology;

Fig. 1

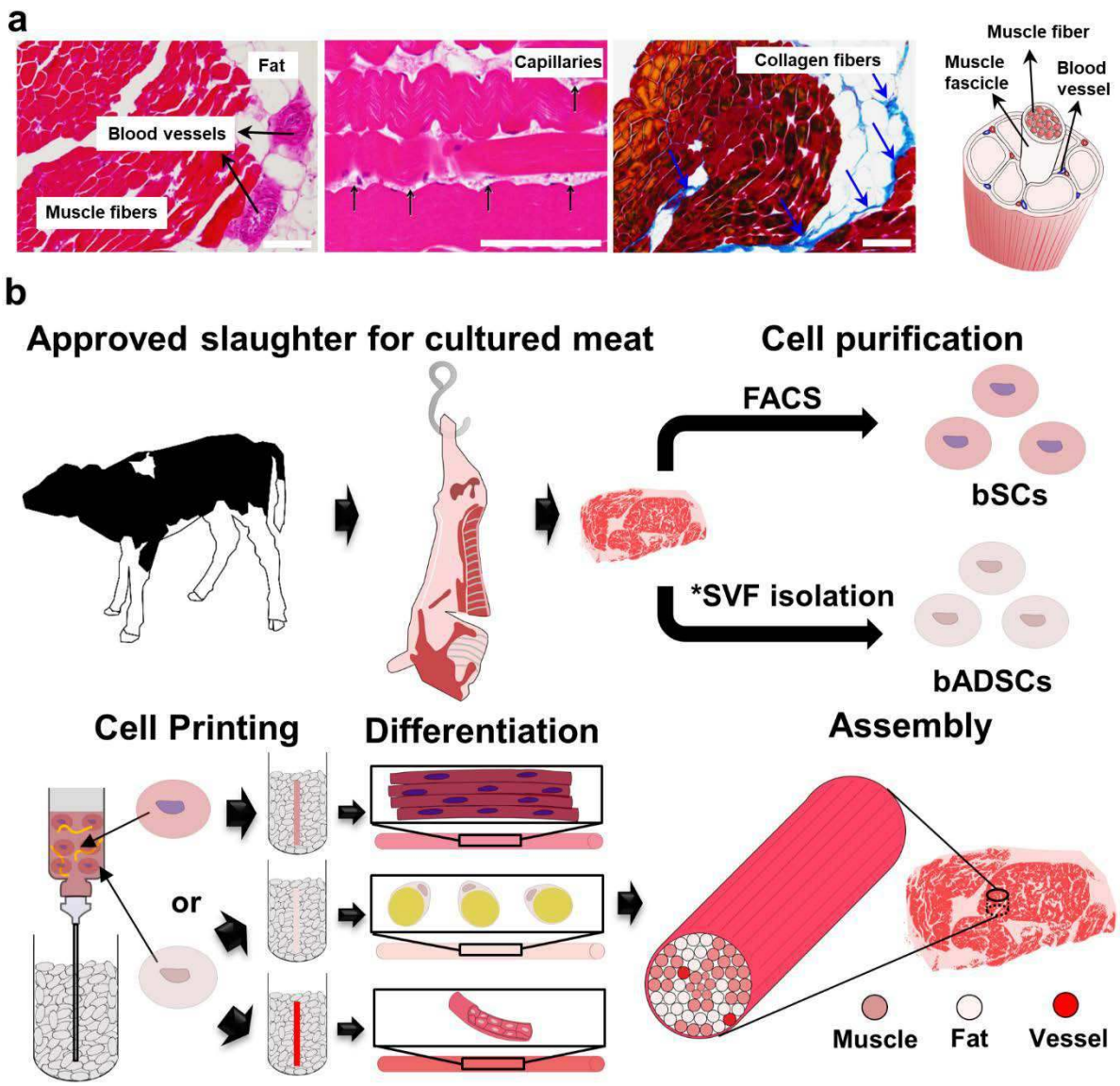
a
Fat
Blood vessels
Muscle fibers
Capillaries
Collagen fibers
Muscle fiber
Muscle fascicle
Blood vessel
b
Approved slaughter for cultured meat
Cell purification
FACS
bSCs
*SVF isolation
bADSCs
Cell Printing
Differentiation
Assembly
or
Muscle
Fat
Vessel

Fig. 2

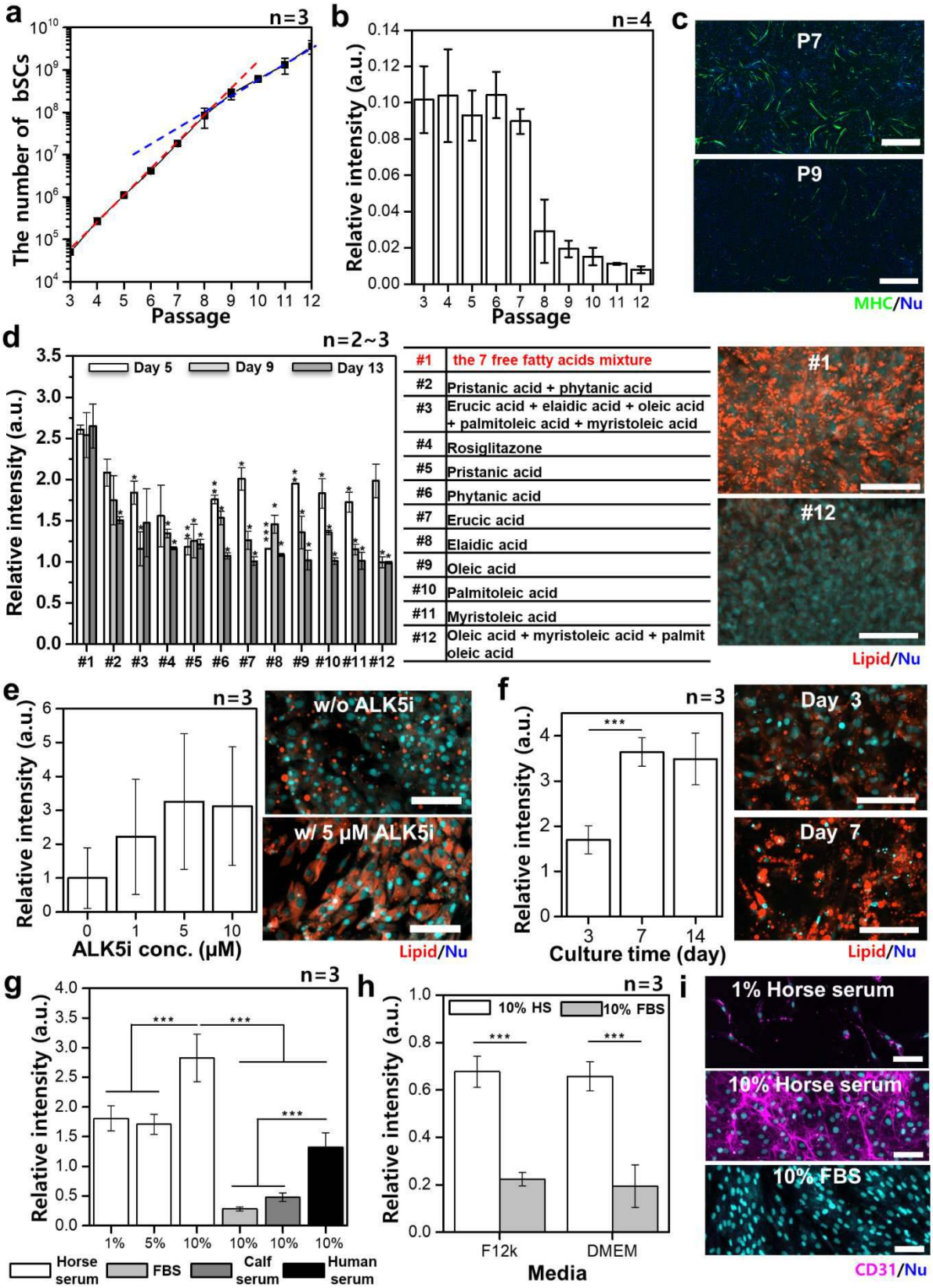
a
n=3
The number of bSCs
Passage
b
n=4
Relative intensity (a.u.)
Passage
c
P7
P9
MHC/Nu
d
n=2~3
Day 5
Day 9
Day 13
Relative intensity (a.u.)
#1 the 7 free fatty acids mixture
#2 Pristanic acid + phytanic acid
#3 Erucic acid + elaidic acid + oleic acid + palmitoleic acid + myristoleic acid
#4 Rosiglitazone
#5 Pristanic acid
#6 Phytanic acid
#7 Erucic acid
#8 Elaidic acid
#9 Oleic acid
#10 Palmitoleic acid
#11 Myristoleic acid
#12 Oleic acid + myristoleic acid + palmit oleic acid
#1
#12
Lipid/Nu
e
n=3
Relative intensity (a.u.)
ALK5i conc. (μM)
w/o ALK5i
w/ 5 μM ALK5i
Lipid/Nu
f
n=3
Relative intensity (a.u.)
Culture time (day)
Day 3
Day 7
Lipid/Nu
g
n=3
Relative intensity (a.u.)
Horse serum
FBS
Calf serum
Human serum
h
n=3
10% HS
10% FBS
Relative intensity (a.u.)
F12k
DMEM
Media
i
1% Horse serum
10% Horse serum
10% FBS
CD31/Nu

Fig. 3

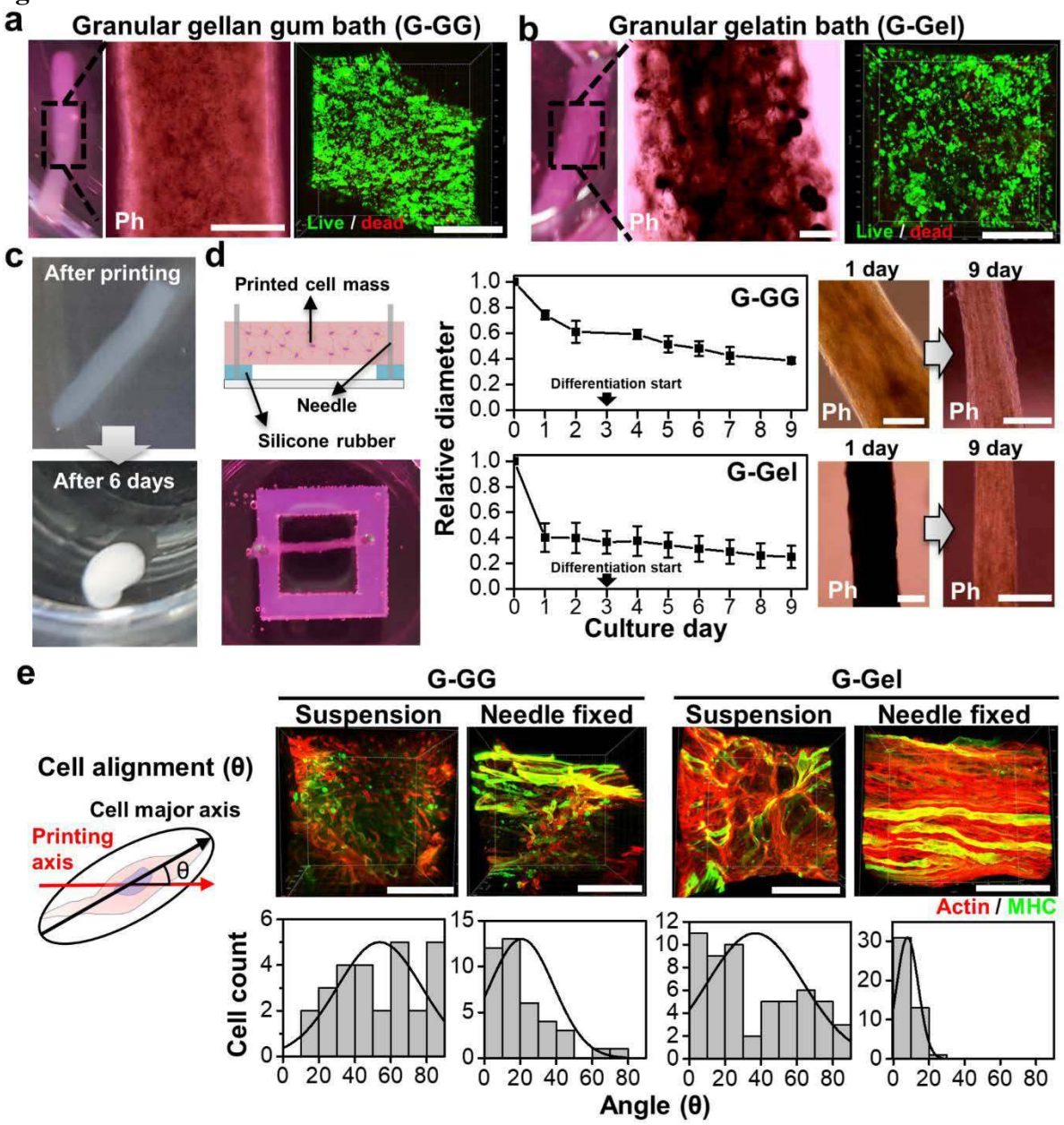
a
Granular gellan gum bath (G-GG)
Ph
Live / dead
b
Granular gelatin bath (G-Gel)
Ph
Live / dead
c
After printing
After 6 days
d
Printed cell mass
Needle
Silicone rubber
G-GG
G-Gel
Differentiation start
Relative diameter
Culture day
1 day
9 day
Ph
e
G-GG
G-Gel
Suspension
Needle fixed
Cell alignment (θ)
Cell major axis
Printing axis
θ
Actin / MHC
Cell count
Angle (θ)

Fig. 4

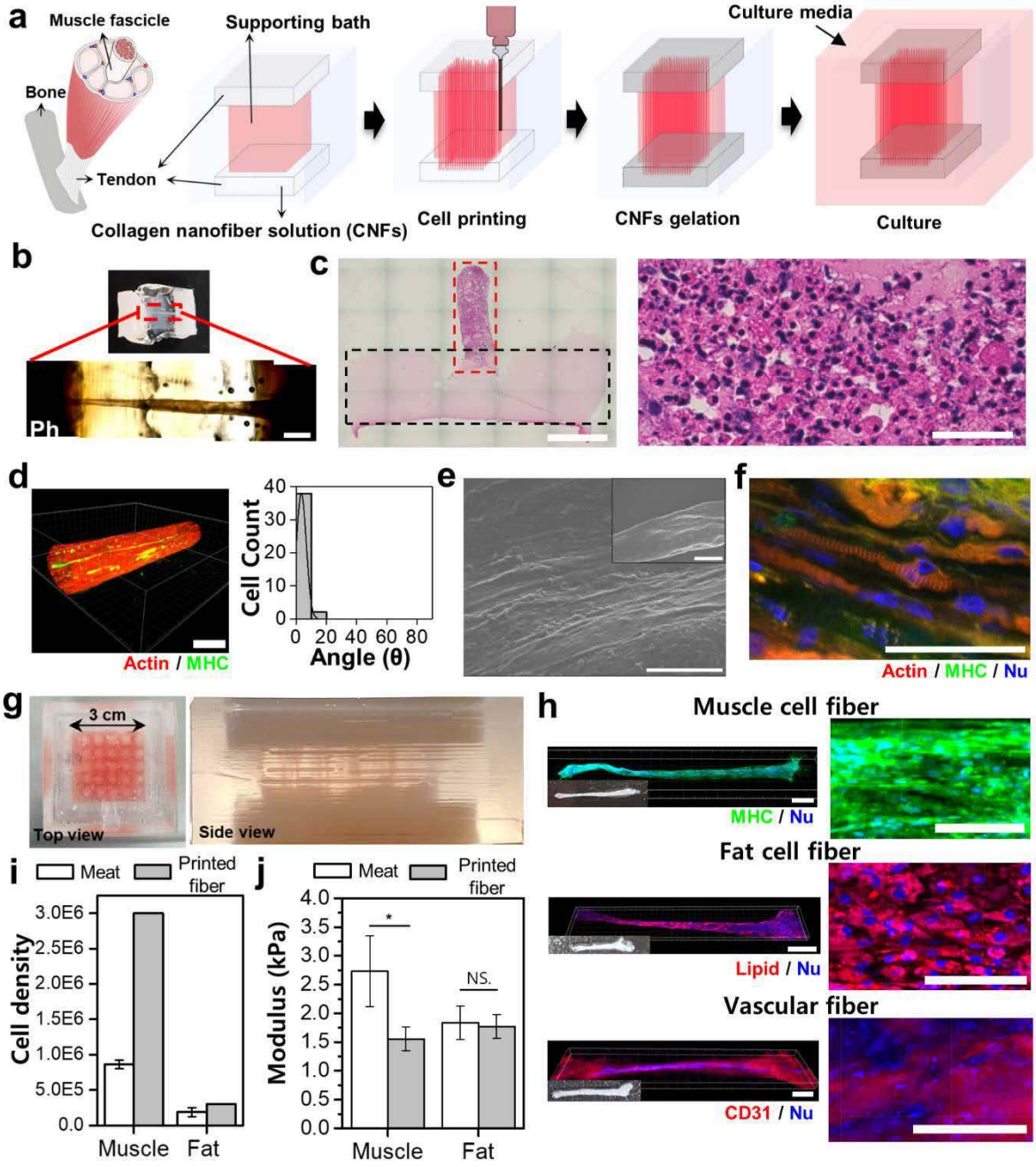
a
Muscle fascicle
Bone
Tendon
Supporting bath
Collagen nanofiber solution (CNFs)
Cell printing
CNFs gelation
Culture media
Culture
b
Ph
c
d
Actin / MHC
Cell Count
Angle (θ)
e
f
Actin / MHC / Nu
g
3 cm
Top view
Side view
h
Muscle cell fiber
MHC / Nu
Fat cell fiber
Lipid / Nu
Vascular fiber
CD31 / Nu
i
Meat
Printed fiber
Cell density
Muscle
Fat
j
Meat
Printed fiber
Modulus (kPa)
*
NS.
Muscle
Fat

Fig. 5

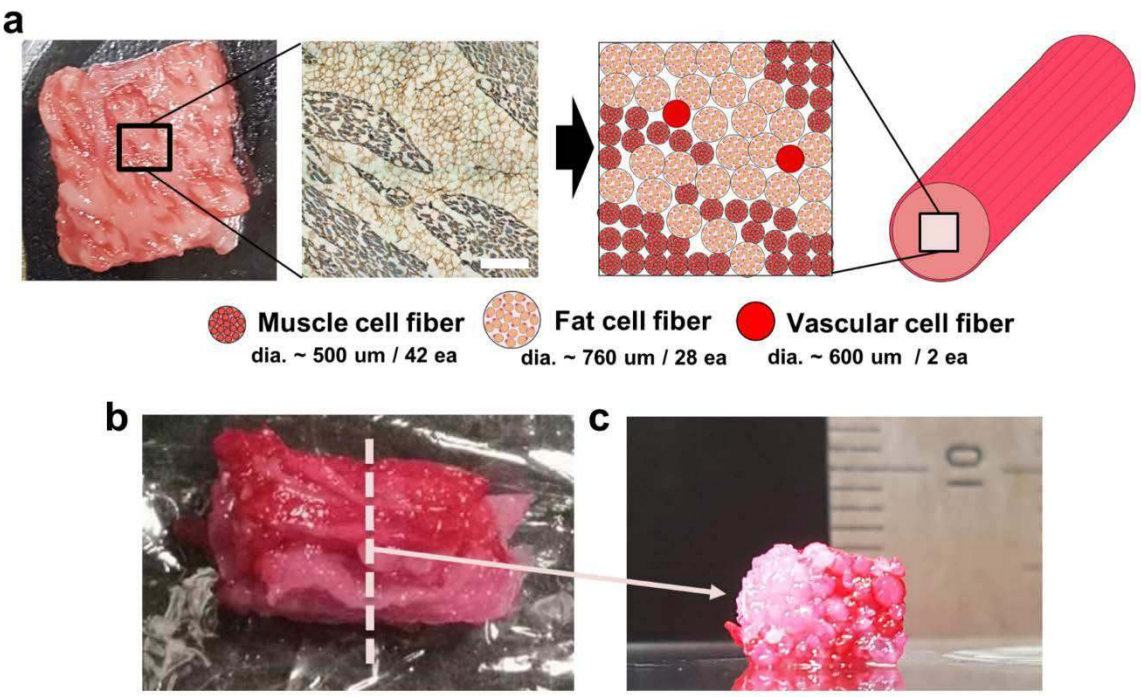
a
Muscle cell fiber
dia. ~ 500 um / 42 ea
Fat cell fiber
dia. ~ 760 um / 28 ea
Vascular cell fiber
dia. ~ 600 um / 2 ea
b
c

Figures

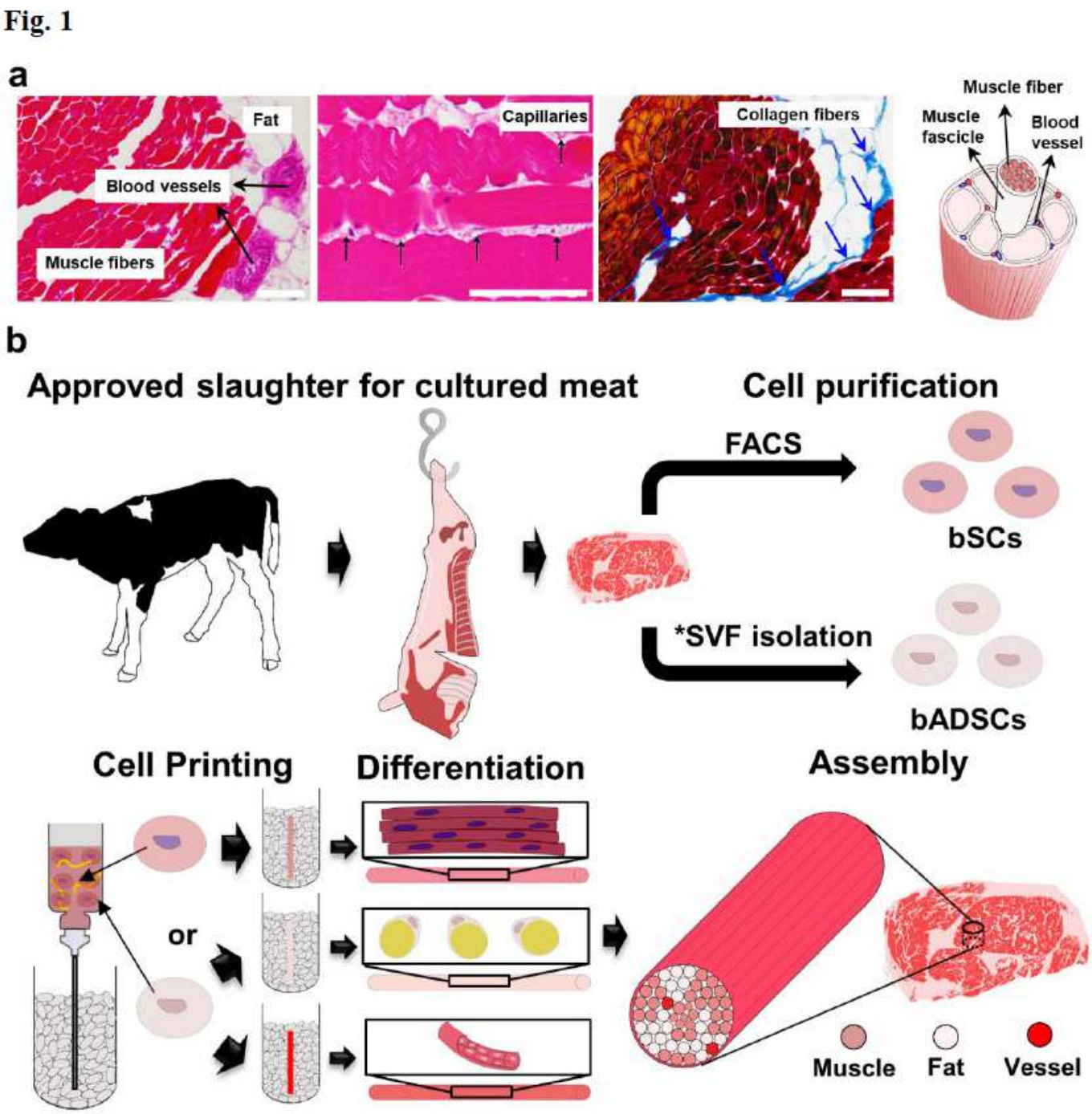

Figure 1

Overview of work a, Structure of steak. (-) H&E- and () Azan-stained images of a piece of steak. All scale bar denotes 100 μm () Schematic of hierarchical structure in muscle. b, Schematic of the construction process for cultured steak. The first step is cell purification of tissue from cattle to obtain bovine satellite cells (bSCs) and bovine adipose-derived stem cells (bADSCs). Second is supporting bath assisted printing (SBP) of bSCs and bADSCs to fabricate the muscle, fat, and vascular tissue with a

fibrous structure. The third is the assembly of cell fibers to mimic the commercial steak's structure. *SVF: stromal vascular fraction

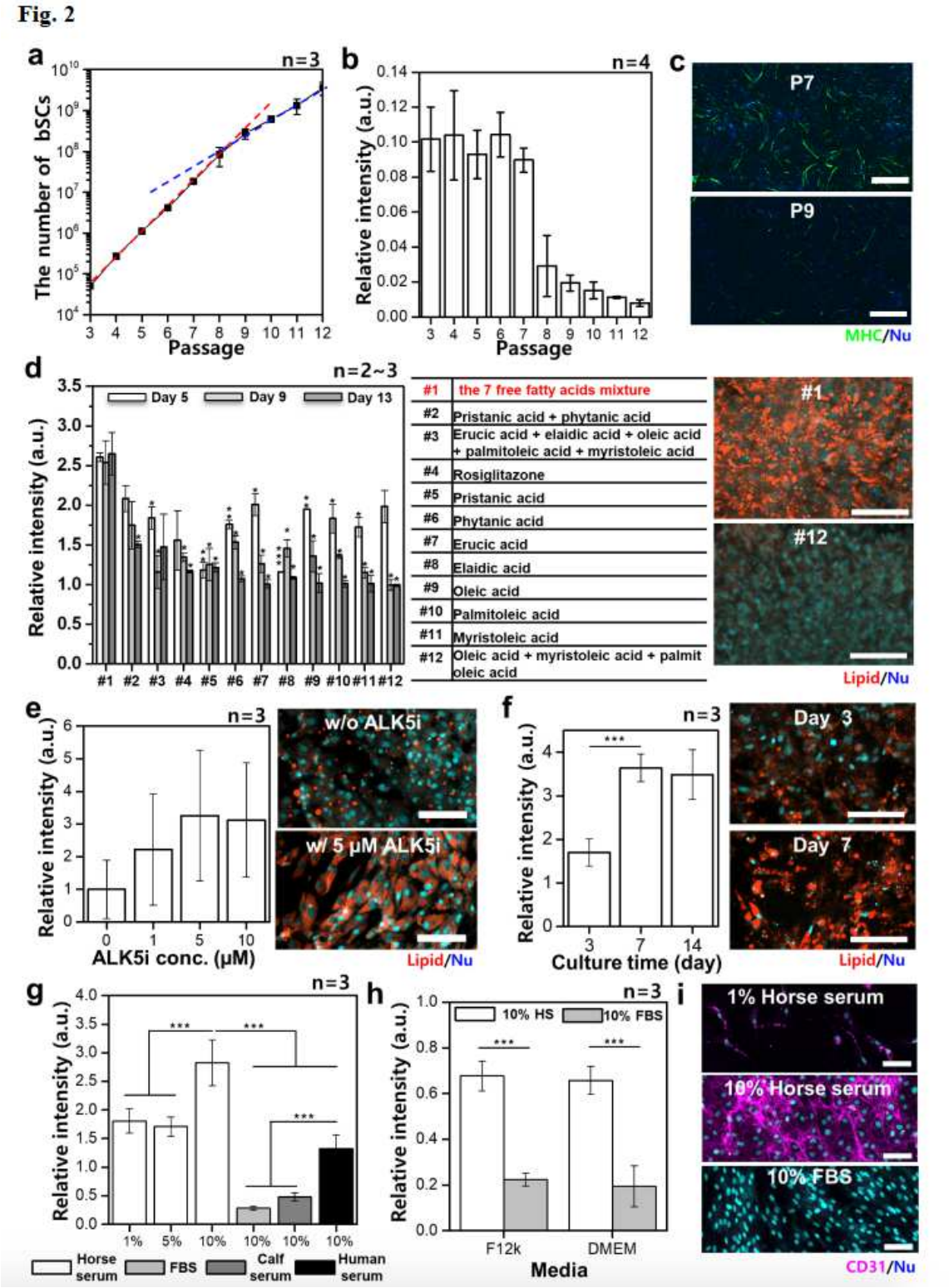

Figure 2

Verification of purified bovine stem cells. a-b, Proliferation rate (a) and differentiation ratio on day 5 of differentiation (b) of bSCs from passage 3 (P3) to P12 cultured on a tissue culture plate. Red line and blue line are a slope from P3 to P8 and from P8 to P12, respectively. c, Representative fluorescence

images of differentiation induced bSCs at P7 and P9 stained for myosin heavy chain (MHC) (green) and nucleus (blue). Scale bars, 1 mm. d, Adipogenesis ratio (left) of 3D gel drop cultured bADSCs derived by 12 combinations of free fatty acids (middle) in DMEM on day 3, 9, and 13 and representative fluorescence images (right) of differentiation induced bADSCs by #1 and #12 combinations of fatty acid on day 13 (red: lipid & blue: nucleus). Statistical significance was calculated with 2-ways ANOVA with Tukey multiple comparison test, n=12 drops tissues/per condition and 2 pictures per drop. Scale bars, 100 μm. e-f, Adipogenesis ratio (left) and representative fluorescence images (right) of 3D gel drop cultured bADSCs depending on the concentration of ALK5i on day 7 (e) and culture day (f) in the #1 combination of free fatty acids (red: lipid & blue: nucleus). Statistical significance was calculated with 1-way ANOVA with Tukey multiple comparison tests, n=2-3 drops tissues/per condition. Scale bars, 100 μm. g-h, Vasculogenesis ratio of bADSCs depending on serum conditions in DMEM (g) and base media (h) on day 7 (magenta: CD31 & blue: nucleus). Statistical significance was calculated with 1-way ANOVA with Tukey multiple comparison test, n=3 different wells/condition, 3 pictures/well. i, Representative fluorescence images of bADSCs depending on serum conditions on day 7 stained for CD31 (magenta) and nucleus (blue). Scale bars, 1 mm. The used bADSCs were extracted from subcutaneous fat. *P<0.05, **P<0.01, ***P<0.001; error bars represent mean ± s.d.

Fig. 3

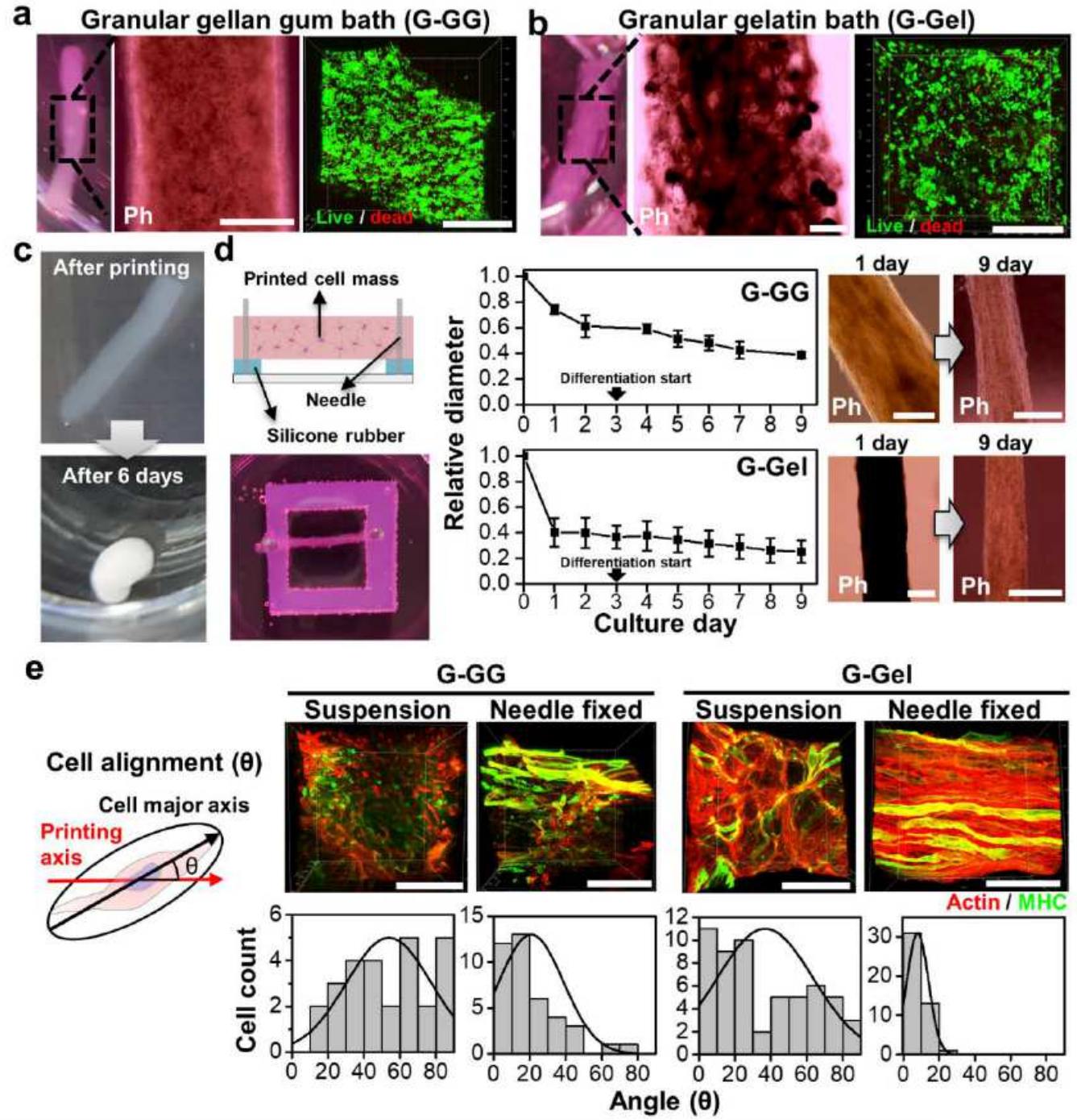

Figure 3

The characterization of bSCs tissue fabricated by SBP. a-b, Optical (left), phase contrast (middle), and fluorescence (right, green: live cells & red: dead cells) images of the bSCs tissues printed inside granular gellan gum (G-GG) (a) and granular gelatin (G-Gel) (b) followed by bath removal. Scale bars, 500 μm. c, Shape change of bSCs tissue fabricated by SBP inside G-Gel from the fibrous form right after printing and bath removal to globular form on day 6 of suspension culture. d, Schematic (left), size change in accordance with culture day (middle), and phase-contrast images (right) of needle fixed culture of printed

bSCs tissues. Error bars represent mean ± s.d. Scale bars, 500 μm. e, Fluorescence images (upper, red: actin & green: MHC) and cell alignment measurements (lower) of the bSCs tissues printed inside G-GG and G-Gel and in suspension and needle fixed cultures on day 3 of differentiation, respectively. Scale bars, 200 μm.

Fig. 4

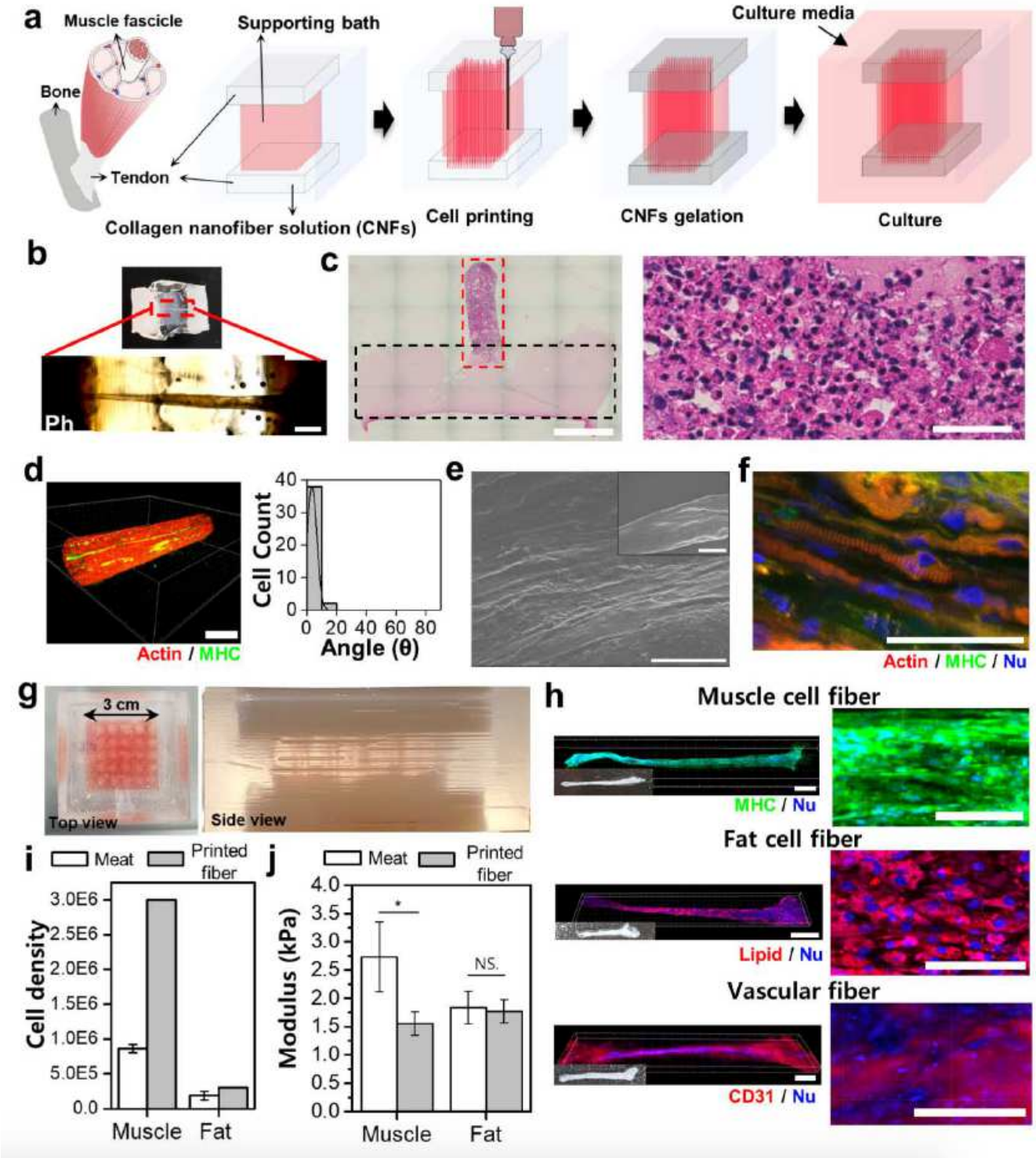

Figure 4

Tendon integrated bioprinting (TIP) for muscle, fat, vascular tissue fabrication. a, The schematic of TIP for cell printing. b, Optical (upper) and phase-contrast (lower) images of the bSCs tissue printed by TIP, keeping the fibrous structure on day 3. The images were taken after fixation. Scale bar, 1 mm. c, The H&E stained image of half of collagen gel (dotted black line) - fibrous bSCs tissue (dotted red line) and a magnified image of the fibrous bSCs tissue (right). Scale bars, 2 mm (left) and 50 μm (right). d, 3D fluorescence image (left) and cell alignment measurement (right) of the TIP-derived bSCs tissue stained with actin (red) and MHC (green) on 3 day of differentiation. Scale bar, 50 μm. e, SEM images of TIP-derived bSCs tissue on 3 day of differentiation. Scale bars, 10 μm & 100 μm (inset). f, Fluorescence image of TIP-derived bSCs tissue stained with actin (red), MHC (green), and nucleus (blue) on 14 day of differentiation. A scale bar, 50 μm. g, The optical images of multiple tissue fabrication (25 ea.) by large-scale TIP. h, Whole fluorescence (left), optical (inset), and magnified (right) images of muscle (on day 4 of differentiation, green: MHC & blue: nucleus), fat (on day 7 of differentiation, red: lipid & blue: nucleus), and vascular (on day 7, red: CD31 & blue: nucleus) tissues fabricated by TIP. Scale bars, 1 mm (left) and 100 μm (right). i-j, Cell concentrations (Calculated values in TIP-derived) (i) and compressive modulus (j) of muscle and fat fibers in the commercial meat and TIP-derived. Statistical significance was calculated with 1-way ANOVA with Tukey multiple comparison test. *P<0.05; error bars represent mean ± s.d.

Fig. 5

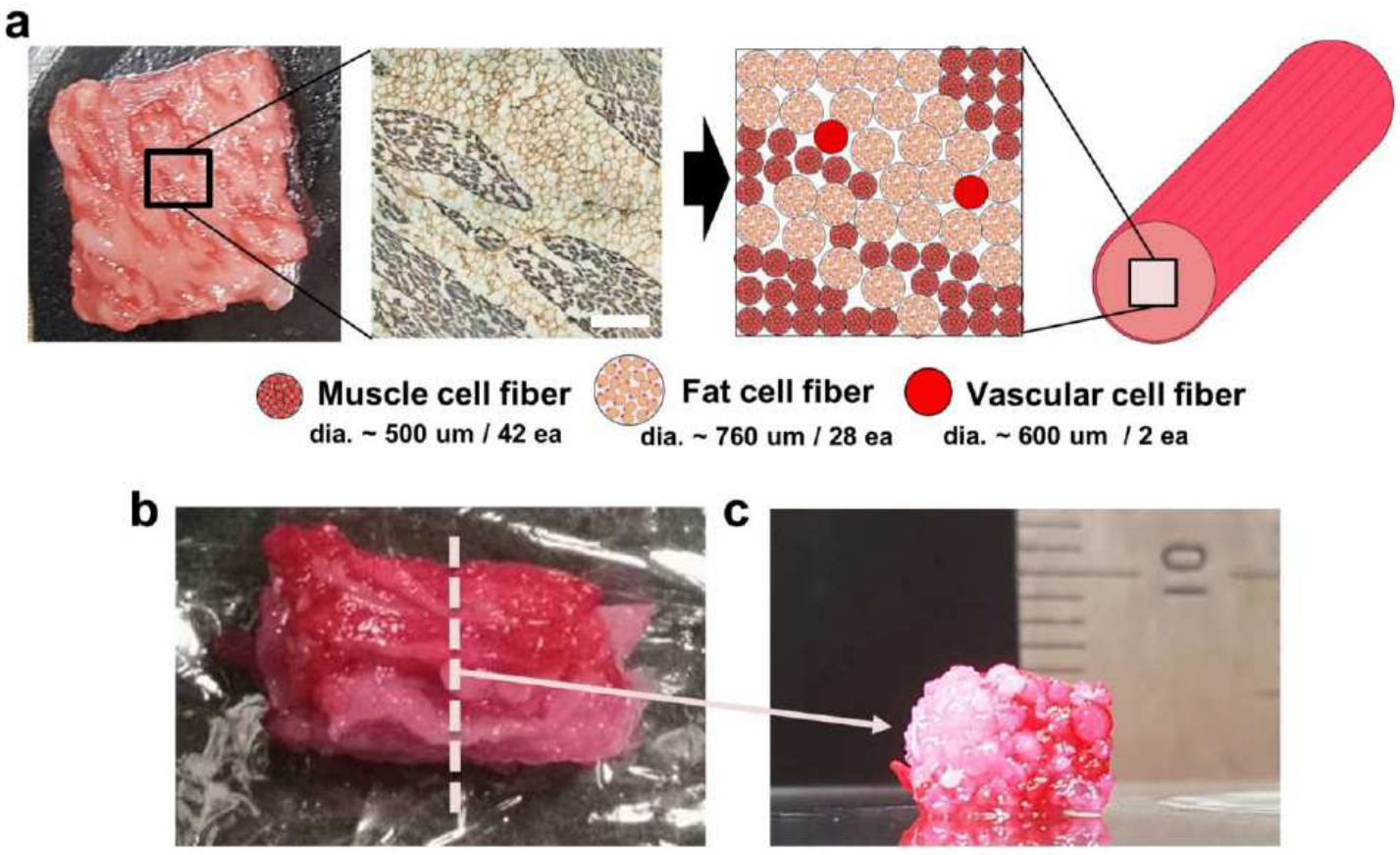

Figure 5

Assembly of fibrous muscle, fat, and vascular tissues to cultured steak. a, Assembly schematic (right) based sarcomeric α-actinin (blue) & laminin (brown) stained image (left) of the commercial meat (Wagyu). It is assumed that the diameter of the fibrous muscle, fat, and vascular tissues are about 500, 760, and 600 μm, respectively. Scale bar, 1 mm. b-c, Optical images of the cultured steak by assembling muscle (42 ea.), fat (28 ea.), and vascular (2 ea.) tissues at (b) top and (c) cross-section view of the dotted line area. Muscle and vascular tissue were stained with carmine (red color), but fat tissue was not.

Supplementary Files

This is a list of supplementary files associated with this preprint. Click to download.

- KangetalCulturedwholecutmeatSI.pdf
- SupplementaryMovie1.mov
- SupplementaryMovie2.mov
- SupplementaryMovie3.mov
- SupplementaryMovie4.mov
- SupplementaryMovie5.mov
- SupplementaryMovie6.mov
- SupplementaryMovie7.mov
- SupplementaryMovie8.mov